nature catalysis

Article

https://doi.org/10.1038/s41929-024-01149-w

Biocatalytic, enantioenriched primary amination of tertiary C–H bonds

Received: 17 August 2023

Accepted: 15 March 2024

Published online: 3 May 2024

Check for updates

Runze Mao[1,4], Shilong Gao[1,4], Zi-Yang Qin[1,4], Torben Rogge[2,3], Sophia J. Wu[1], Zi-Qi Li[1], Anuvab Das[1], K. N. Houk[2] & Frances H. Arnold[1]

Intermolecular functionalization of tertiary C–H bonds to construct fully substituted stereogenic carbon centres represents a formidable challenge: without the assistance of directing groups, state-of-the-art catalysts struggle to introduce chirality to racemic tertiary sp^3-carbon centres. Direct asymmetric functionalization of such centres is a worthy reactivity and selectivity goal for modern biocatalysis. Here we present an engineered nitrene transferase (P411-TEA-5274), derived from a bacterial cytochrome P450, that is capable of aminating tertiary C–H bonds to provide chiral α-tertiary primary amines with high efficiency (up to 2,300 total turnovers) and selectivity (up to >99% enantiomeric excess). The construction of fully substituted stereocentres with methyl and ethyl groups underscores the enzyme's remarkable selectivity. A comprehensive substrate scope study demonstrates the biocatalyst's compatibility with diverse functional groups and tertiary C–H bonds. Mechanistic studies explain how active-site residues distinguish between the enantiomers and enable the enzyme to perform this transformation with excellent enantioselectivity.

Direct enantioselective functionalization of C(sp^3)–H bonds is an ideal approach to synthesize high-value-added chiral molecules from the viewpoints of atom and step economy[1–5]. In recent years, many powerful catalytic methods have been developed towards this goal, with notable advances made for enantioselective functionalization of secondary C–H bonds (Fig. 1a)[1–10]. By contrast, intermolecular asymmetric functionalization of racemic tertiary C–H bonds, particularly those with a the logarithmic scale of the acid dissociation constant (pK_a)> 25 and in the absence of directing groups, towards the formation of fully substituted sp^3-carbon stereocentres remains unexplored in synthetic chemistry (Fig. 1b). The challenges of this transformation include the difficulty of precisely recognizing three different substituents attached to a tertiary carbon centre (Fig. 1b), especially when those substituents have only subtle steric and/or electronic differences; the lack of an intermolecular counterpart to recent breakthroughs in intramolecular enantioselective tertiary C–H functionalizations[11–15] and, finally, potential steric clash between the catalyst and the tertiary carbon. Chemists often achieve precise facial recognition by strategically incorporating bulky substituents or functional groups into a chiral catalyst. However, when it comes to the functionalization of a tertiary C–H bond, the steric clash between the bulky catalyst and the crowded surrounding of a tertiary carbon inhibits the approach of the catalyst to the tertiary C–H bond. Consequently, a trade-off arises between increasing the catalyst's steric bulk to better control stereoselectivity and decreasing it to avoid a steric clash with the tertiary sp^3-carbon surroundings (Fig. 1b).

Unlike small-molecule catalysts, enzymes have large, three-dimensional (3D) structures determined by the folding of their polypeptide chain(s). With precisely sculpted 3D structures, enzymes can differentiate steric and electronic nuances as subtle as those between methane and ethane molecules[16]. With precise adjustments of their folded structures, enzymes can also achieve excellent stereoselectivity while maintaining high activity by avoiding severe steric clashes with bulky substrates[17]. We thus consider enzyme catalysis to be a promising approach to tackle existing challenges in the enantioselective functionalization of tertiary C–H bonds.

[1]Division of Chemistry and Chemical Engineering, California Institute of Technology, Pasadena, CA, USA. [2]Department of Chemistry and Biochemistry, University of California, Los Angeles, CA, USA. [3]Present address: Institut für Chemie, Technische Universität Berlin, Berlin, Germany. [4]These authors contributed equally: Runze Mao, Shilong Gao, Zi-Yang Qin. e-mail: frances@cheme.caltech.edu

https://doi.org/10.1038/s41929-024-01149-w

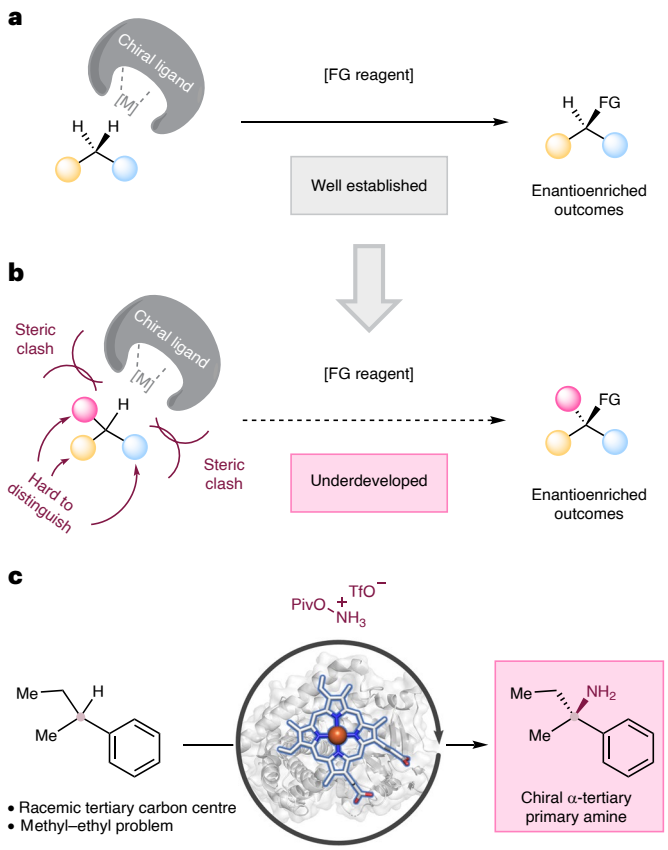

Fig. 1 | Direct enantioselective functionalization of C(sp^3)–H bonds. **a**, General scenario for intermolecular enantioselective functionalization of secondary carbon centres. Secondary carbons offer less steric hindrance, which facilitates the construction of chirality. This type of transformation has been well documented. **b**, General scenario for intermolecular enantioselective functionalization of tertiary carbon centres. Tertiary carbons that possess chiral centres are difficult for catalysts to approach and recognize. This type of transformation is rarely reported. **c**, This work: biocatalytic, enantioselective primary amination of tertiary C–H bonds. M, metal catalysts; FG, functional groups; Piv, pivaloyl.

Cytochromes P450 represent nature's most prevalent catalysts for C–H functionalization[10], with enzymes from this vast family directly activating C–H bonds for a wide range of oxidative transformations[18]. Furthermore, cytochromes P450 are excellent candidates for directed evolution and discovery of non-natural activities due to their structural flexibility and remarkable promiscuity[19]. Several reports have demonstrated abiological C–H functionalizations achieved by expanding the catalytic repertoire of the iron-haem-containing cytochrome P450 family[8,9,20]. The activity and selectivity of these biocatalytic C–H functionalizations frequently complement state-of-the-art methodologies based on small-molecule catalysts, making them valuable additions to the synthetic chemist's toolbox[8,21]. Motivated by these precedents, we sought to leverage these enzymes for enantioselective intermolecular functionalization of tertiary C–H bonds.

Given the widespread presence of α-tertiary amines in bioactive compounds[22], the initial focus was on the primary amination of tertiary C–H bonds. Despite the existence of many methods for synthesizing chiral α-tertiary amines with stoichiometric amounts of auxiliary reagents, such as Ellman's sulfinamides[23,24], catalytic strategies for enantioselective conversion of substrates into chiral α-tertiary amines are rare[11–13,22,25], because classical methods for synthesizing chiral α-secondary amines, including asymmetric reduction of imines[26], biocatalytic transamination[27] and reductive amination[28], are not applicable to the synthesis of chiral α-tertiary amines due to the absence of protons in the fully substituted carbon centre. From a retrosynthetic perspective, intermolecular amination of tertiary C–H bonds provides an ideal and straightforward method for the assembly of chiral α-tertiary amines (Fig. 1c). The Arnold group recently reported primary amination of these tertiary C–H bonds, but all the products were non-chiral[29,30]. Here we present a biocatalytic system that exhibits remarkable ability to aminate tertiary C–H bonds, providing high-value chiral α-tertiary primary amines with exceptional efficiency and selectivity.

Results

Initial discovery and evolution of tertiary C–H primary aminase P411-TEA-5274

We initiated the study by testing the coupling of *sec*-butylbenzene **1a** and hydroxylamine ester **2a** (Fig. 2a) catalysed by an in-house collection of engineered cytochromes P411 (serine-ligated cytochrome P450 variants). These reagents were chosen for several reasons: first, compared to the elaborated starting materials used for many other tertiary C–H functionalizations, **1a** is simple, inexpensive and readily available[11–15]. Second, the tertiary carbon centre of **1a** is racemic and attaches to a methyl and an ethyl substituent; distinguishing these is notoriously difficult in asymmetric catalysis[11,31,32]. Last, hydroxylamine ester **2a** has recently been shown to serve as a nitrene precursor for haemoprotein-catalysed secondary C–H primary amination[29]; we wanted to expand that demonstration to primary amination of tertiary C–H bonds.

A panel of 48 cytochromes P411 previously engineered for nitrene transformations was screened in whole *Escherichia coli* cells against **1a** and **2a** under anaerobic conditions (Fig. 2). The resulting reaction mixtures were monitored and analysed after 20 h for the formation of α-tertiary primary amine **3a**. Variant P411-TEA-5267 (tertiary C–H primary aminase), which has three mutations (C324L, N395R and G438V) with respect to $P411_{BPA}$ (previously engineered for benzylic C–H primary amination)[29], produced the desired product **3a** with a total turnover number (TTN) of 20 (Fig. 2b; 1% yield, Supplementary Table 1). The primary amine **3a** synthesized by P411-TEA-5267 was determined to have excellent stereopurity, with 90% enantiomeric excess (e.e.).

P411-TEA-5267 served as the starting point for directed evolution. Sequential rounds of site-saturation mutagenesis (SSM)[33,34] and screening were performed to improve catalytic activity towards synthesis of **3a**. We referred to the crystal structure of related P411 variant **E10** (ref. 35) (haem domain only) and mainly targeted for mutagenesis amino acid residues proximal to the haem cofactor and/or residing on flexible loops, or those distal sites that have been shown to play an important role in enhancing abiological carbene and nitrene transfer activities (Fig. 2c)[8]. During each round of SSM, enzyme libraries were generated and screened for product formation in 96-well plates in the form of bacterial whole-cell catalysts. Three rounds of SSM and screening introduced mutations M354E, R395S and A327V, leading to a threefold improvement of the TTN from 20 to 64 (Fig. 2b,d). Subsequent rounds of evolution introduced the M177Y and S72T mutations on the α-helices above the haem cofactor, as well as the A399G mutation on the loop directly below the haem cofactor. These mutations boosted the activity more than twofold, reaching 140 TTN (Fig. 2). The Q403A mutation located on the α-helix below the haem cofactor doubled the enzyme activity to 270 TTN (Fig. 2). On re-evaluation of position 395 in the loop beneath the haem cofactor, we found the S395V mutation increased the enzyme's activity almost fourfold to 970 TTN (26% yield, Supplementary Table 2), culminating in the final variant, P411-TEA-5274 (Fig. 2). In the standard conditions, an oxygen depletion system (catalase and glucose oxidase) was introduced to ensure a strict anaerobic environment. However, in the absence of this oxygen depletion system the yield and TTN only decrease slightly (entries 8 and 10, Supplementary Table 2), demonstrating the synthetic utility of this biotransformation. Notably, the enzyme's enantioselectivity towards the formation of **3a**

https://doi.org/10.1038/s41929-024-01149-w

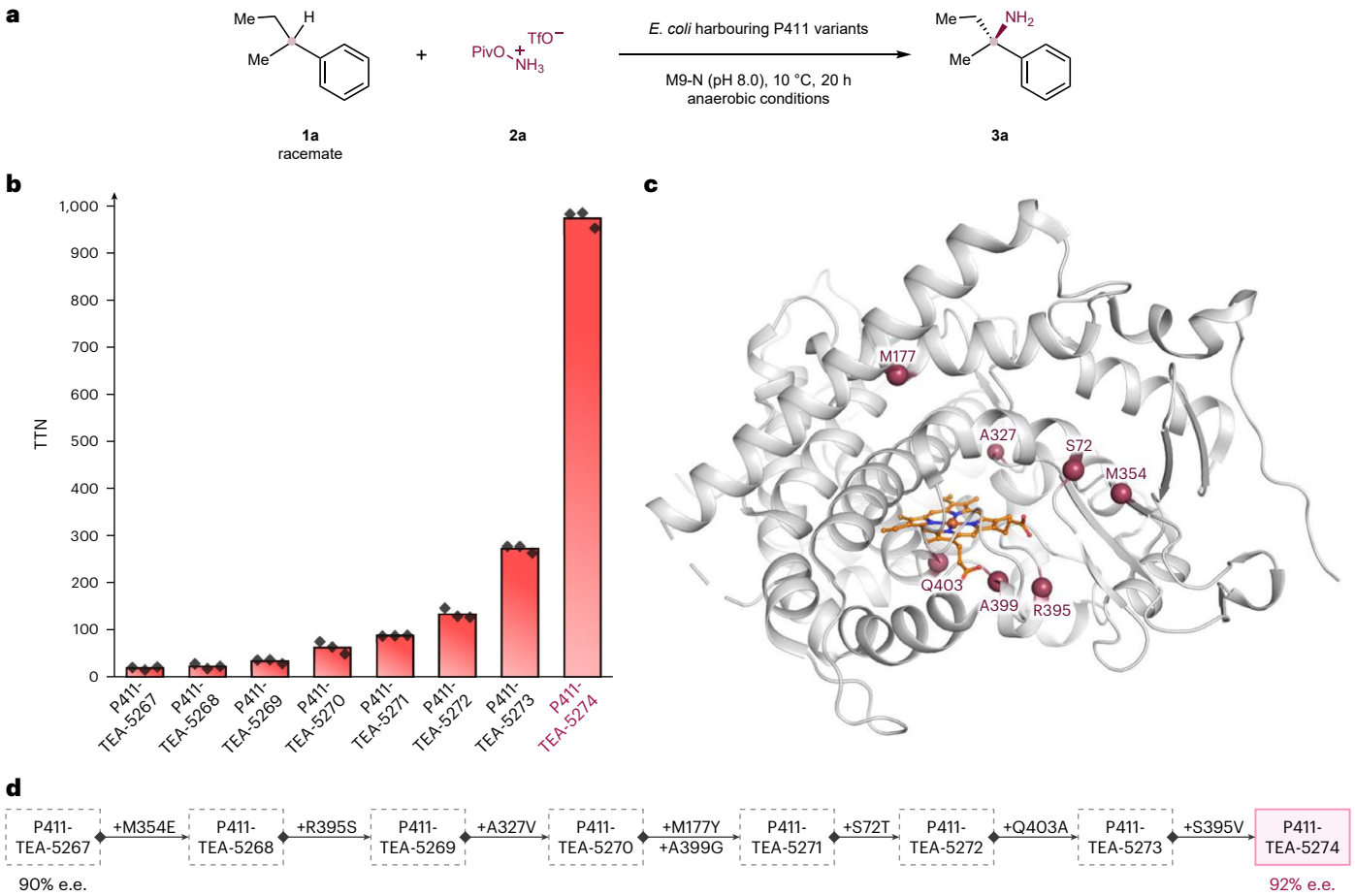

Fig. 2 | Directed evolution for enzymatic primary amination of tertiary C–H bonds. a, Reaction conditions: 5 mM **1a**, 10 mM **2a**, *E. coli* whole cells harbouring P411 variants (OD_{600} = 30) in M9-N aqueous buffer (pH 8.0), 5% (v/v) EtOH (cosolvent), 10 °C, anaerobic conditions, 20 h. **b**, Evolution trajectory of tertiary C–H primary aminase (P411-TEA) for the synthesis of α-tertiary primary amine **3a**. **c**, The mutations (S72, M177, A327, M354, R395, A399 and Q403) that enhance activity or enantioselectivity are highlighted in the active site of closely related P411 variant **E10** (Protein Data Bank ID 5UCW)[35]. **d**, Summary of beneficial mutations leading to P411-TEA-5274. TTN is defined as the (molar) amount of indicated product divided by the amount of haem protein in the reaction, as measured by the haemochrome assay (see Supplementary Method 7 for more details). Yields were calculated from high-performance liquid chromatography calibration curves and the average of triplicate experiments (n = 3).

also improved slightly during the evolution campaign, increasing from 90% e.e. (P411-TEA-5267, Fig. 2d) to 92% e.e. (P411-TEA-5274, Fig. 2d).

Substrate scope study of tertiary C–H primary aminase P411-TEA-5274

With C–H primary aminase P411-TEA-5274 in hand, we proceeded to explore its performance on various substrates (Fig. 3). Representative substrates were designed with mixed kinds of C–H bond (**1a**, Fig. 3) and with diverse spatial hindrances (**1a** and **1c**–**1e**, Fig. 3), electronic effects (**1f**–**1g**, Fig. 3), structures (**1i**–**1j**, Fig. 3) and two different types of tertiary C–H bond (**1k**–**1l**, Fig. 3) to examine the impact of these factors on the activity and selectivity of the enzyme, as well as the enzyme's regional selectivity. We incorporated both methyl and ethyl groups at the tertiary carbon centres of most substrates (**1a**, **1c**–**1g** and **1i**–**1l**, Fig. 3)[11,31,32]. These substrates allow us to assess the selectivity of the enzyme in conditions that present considerable challenges for other systems.

To investigate enzyme regioselectivity, we tested substrate **1a** (Fig. 3). Substrate **1a** has an sp^3 tertiary C–H bond and sp^2 C–H bonds. Existing reports have demonstrated iron catalysts can efficiently catalyse primary amination of sp^2 C–H bonds[36–38]. By contrast, this enzyme exclusively catalysed the amination of the sp^3 tertiary C–H bond of **1a**, giving **3a** with high efficiency (970 TTN, Fig. 3) and exclusive regioselectivity (>99:1 regioselectivity ratio (r.r.), Fig. 3) and enantioselectivity (92% e.e., Fig. 3). A 1.0 mmol reaction was performed under the standard conditions, and primary amine **3a** could be isolated in 17% isolated yield and with 92% e.e. by using simple acid–base extraction (Fig. 3). Substrates (**1b**–**1d**) possess an sp^3 tertiary C–H bond and sp^3 primary C–H bonds. Although the former has a smaller bond-dissociation energy than the latter[39], the latter is kinetically more favourable for activation. This enzyme aminated the tertiary C–H bond of **1b**–**1d**, delivering **3b**–**3d** with high efficiency (up to 860 TTN). We next installed a methyl group (**1c**) and a methoxy group (**1f**) at the *para*-position of the phenyl ring. The enzyme's activity towards the construction of **3c** and **3f** dropped to 310 and 110 TTN, respectively. However, the enantioselectivities for both compounds were >99% e.e. (Fig. 3). Conversely, when a methyl group was introduced at the *meta*-position of the phenyl ring, the enantioselectivity decreased to 60% e.e., but the enzyme's activity was high (**3d**, 860 TTN, Fig. 3). When a methyl group was introduced at the *ortho*-position, the enzyme struggled to convert **1e** to **3e** (Fig. 3). When a fluoro-substituent was introduced at the *para*-position, the enzyme maintained high enantioselectivity, albeit with decreased activity (**3g**, 95% e.e., 73 TTN, Fig. 3). When aminating an achiral tertiary carbon centre, we found the efficiency was also good (**3h**, 300 TTN, Fig. 3). In addition, when the aryl moiety was replaced with heteroaryl moieties, such as a pyridyl (**1i**) or a thienyl (**1j**) substituent, the enzyme retained satisfactory catalytic activity and good enantioselectivity

https://doi.org/10.1038/s41929-024-01149-w

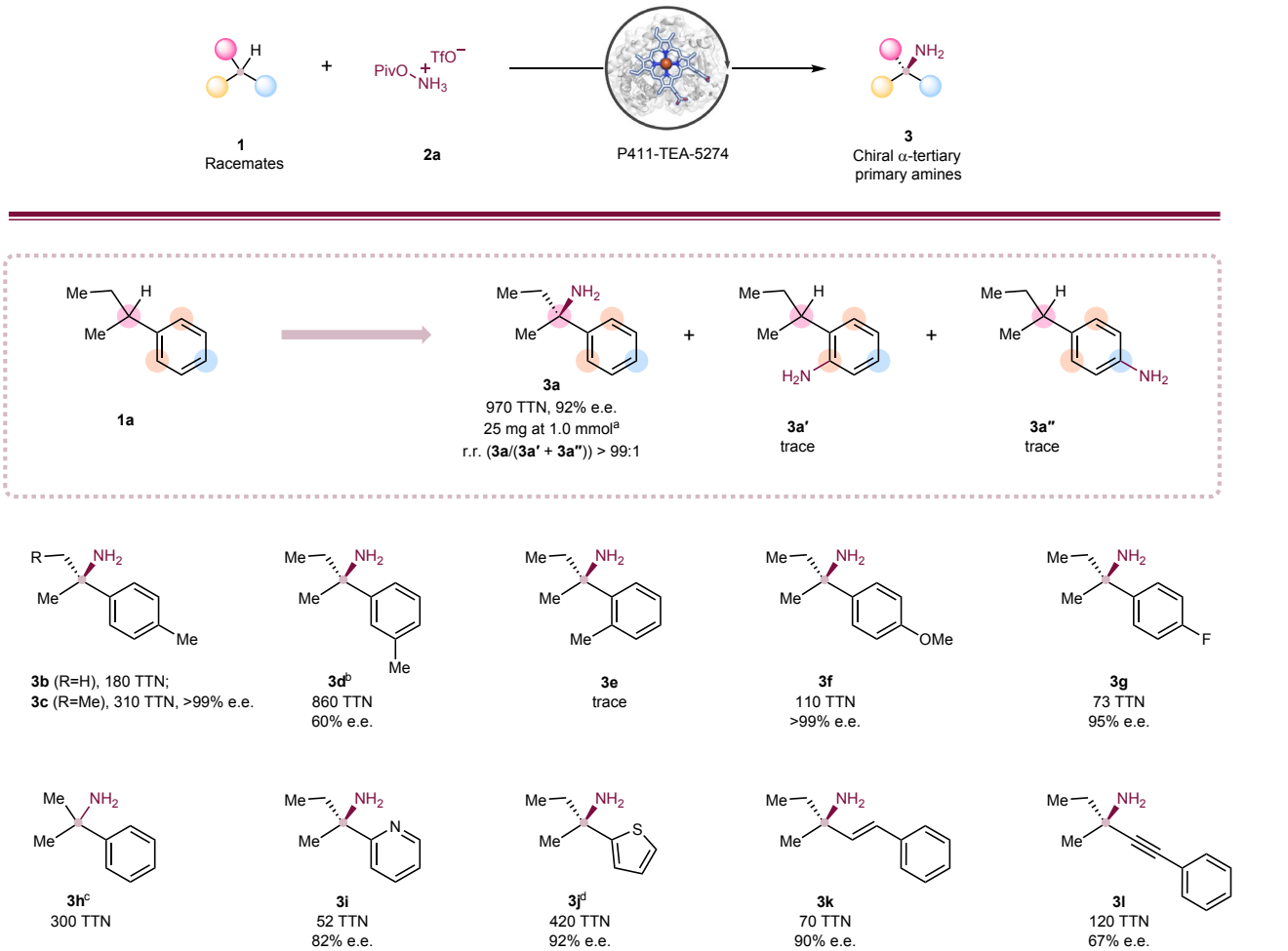

Fig. 3 | Substrate scope study. Reaction conditions were: 5 mM **1a**, 10 mM **2a**, *E. coli* whole cells harbouring P411-TEA-5274 (OD_{600} = 30) in M9-N aqueous buffer (pH 8.0), 5% (v/v) EtOH (cosolvent), 10 °C, anaerobic conditions, 20 h. [a]17% isolated yield at 1.0 mmol scale. [b]16% isolated yield at 0.5 mmol scale. [c]9% isolated yield at 0.5 mmol scale. [d]10% isolated yield at 0.5 mmol scale. TTN is defined as the (molar) amount of indicated product divided by the amount of haem protein in the reaction, as measured by the haemochrome assay (see Supplementary Method 7 for more details). r.r., regioisomeric ratio.

(**3i** (52 TTN, 82% e.e.) and **3j** (420 TTN, 92% e.e.)). Moreover, the biocatalytic system is not only applicable to benzylic tertiary C–H bonds but also to allylic (**3k**, 70 TTN, 90% e.e.) and propargylic tertiary C–H bonds (**3l**, 120 TTN, 67% e.e.). The absolute stereochemistry for enzymatic product **3f** was assigned as *S* by comparing the elution order of the two enantiomers with a literature report[40] and through X-ray crystallography (Supplementary Table 8 and Supplementary Fig. 21). The other α-tertiary primary amines **3** were assigned by analogy.

Experimental and computational study of P411-TEA-5274

To better understand the mechanism of this biotransformation, we designed a series of substrate probes (Fig. 4). First, enantiopure substrates (*R*)-**1f** and (*S*)-**1f** were synthesized (see Supplementary Information for more details) and used to react with **2a** under standard conditions catalysed by P411-TEA-5274 (Fig. 4a,b). Experimental results showed that the efficiency of (*R*)-**1f** transforming into **3f** (420 TTN, Fig. 4a) was much higher (more than 16-fold difference) than that of (*S*)-**1f** transforming into **3f** (26 TTN, Fig. 4b), indicating the enzyme prefers the (*R*)-enantiomer. Moreover, we observed that (*R*)-**1f** was converted to (*S*)-**3f** (>99% e.e.) and (*S*)-**1f** was converted to (*R*)-**3f** (−85% e.e.), indicating that the enzyme achieves enantioselectivity via kinetic resolution and maintains the stereoconfiguration of the favoured enantiomer.

Next, we synthesized substrates that incorporate a stereodefined olefin moiety ((*E*)-**1m** and (*Z*)-**1m**, Fig. 4c,d), and subjected them to enzymatic reactions. Sscrambling of the olefin geometry was observed in the (*Z*)-substrate, with the (*Z*)-substrate yielding a considerable proportion of the scrambled product that harbours a thermodynamically more stable product (*E*)-**3m** (*E*/*Z* > 99:1, Fig. 4d). In line with established literature on related iron-based catalysts[11,41–43], this observed erosion of C=C stereochemistry supports the generation of a carbon-centred radical at the allylic position and a stepwise pathway, contradicting a concerted C–H insertion mechanism.

To understand the rate-determining step of this enzyme-catalysed reaction, the kinetic isotope effect (KIE) between cumene **1b** and cumene-d_7 **1b′** was measured (Fig. 4e,f). The non-competitive KIE was 9.5, while the competitive KIE was 22.9. These results contrast with previously measured KIEs for the benzylic C–H amidation of ethyl benzene[35], while aligning with those for the nitrogen insertion into unactivated C–H bonds[44], suggesting that the hydrogen-atom transfer (HAT) is the rate-limiting step and a higher degree of tunnelling than previously observed in these systems[44].

To gain further insight into the reaction of **1a** with the iron–nitrene intermediate in the active site of the enzyme, molecular dynamics simulations were performed on a mimic of the enantioselectivity-determining HAT transition state, using the closely related P411 enzyme **E10** (ref. 35) as the starting point (beneficial mutations were introduced manually and a restraint was applied to the $N_{nitrene}$–H–$C_{tertiary}$ distance; Supplementary Figs. 22–26). Simulations on the hydrogen-atom transfer with substrate

https://doi.org/10.1038/s41929-024-01149-w

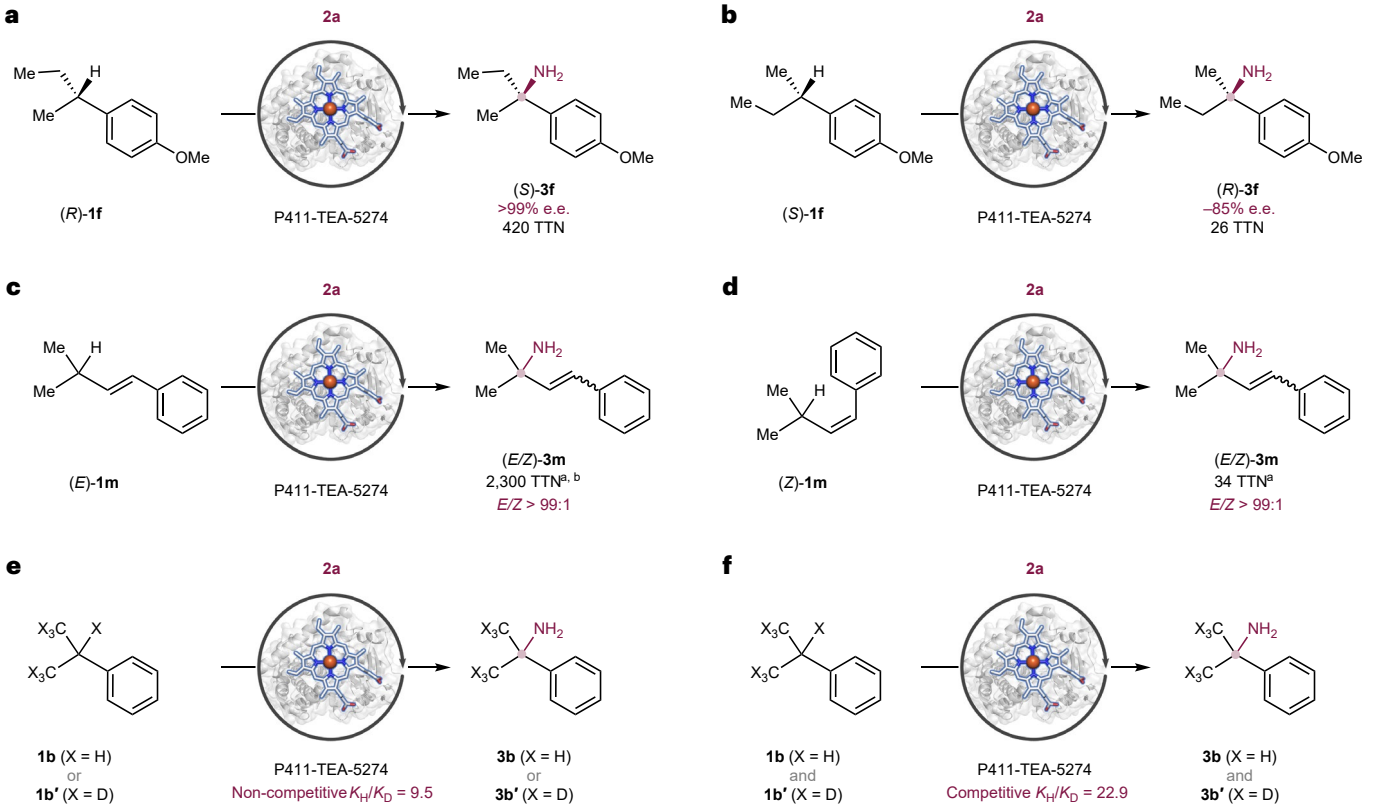

Fig. 4 | Mechanistic studies of enantioenriched enzymatic primary amination of tertiary C–H bonds. a,**b**, Nitrene transfer reactions catalysed by P411-TEA-5274 using (*R*)- (**a**) or (*S*)-**1f** (**b**). Reaction conditions were: 5 mM (*R*)- or (*S*)-**1f**, 10 mM **2a**, *E. coli* whole cells harbouring P411-TEA-5274 (OD_{600} = 30) in M9-N aqueous buffer (pH 8.0), 5% (v/v) EtOH (cosolvent), 10 °C, anaerobic conditions, 20 h. **c**,**d**, Nitrene transfer reactions catalysed by P411-TEA-5274 using (*E*)- (**c**) or (*Z*)-**1m** (**d**). Reaction conditions were 5 mM (*E*)- or (*Z*)-**1m**, 10 mM **2a**, *E. coli* whole cells harbouring P411-TEA-5274 (OD_{600} = 30) in M9-N aqueous buffer (pH 8.0), 5% (v/v) EtOH (cosolvent), 10 °C, anaerobic conditions, 20 h. *E*/*Z* ratios were determined by ^{1}H nuclear magnetic resonance. **e**,**f**, Nitrene transfer reactions catalysed by P411-TEA-5274 using **1b** or **1b′** (d_7-**1b**); non-competitive (**e**) and competitive (**f**). Reaction conditions were: 5 mM **1b** or **1b′**, 10 mM **2a**, *E. coli* whole cells harbouring P411-TEA-5274 (OD_{600} = 30) in M9-N aqueous buffer (pH 8.0), 5% (v/v) EtOH (cosolvent), 10 °C, anaerobic conditions, 20 h. TTN is defined as the (molar) amount of indicated product divided by the amount of haem protein in the reaction, as measured by the haemochrome assay (see Supplementary Method 7 for more details). [a]TTNs were calculated based on all stereoisomers. [b]45% isolated yield at 0.6 mmol scale (Supplementary Method 17).

(*R*)-**1a**, which in the experiment delivers the major enantiomer (*S*)-**3a**, and the other enantiomer (*S*)-**1a** revealed that with both substrates the phenyl-substituent is preferentially oriented towards the left-hand side of the active site, corresponding to an N1-Fe-$N_{nitrene}$-C_{phenyl} dihedral angle of approximately 20° (Fig. 5). In this orientation, the phenyl-substituent is tightly positioned between a number of surrounding hydrophobic residues, with minimum C–C distances as close as 3.5, 3.9 and 3.9 Å between **1a** and A87, A264 and M263, respectively, indicating the possibility of stabilizing C–H–π interactions (see Supplementary Figs. 22 and 23 for details). This tight fit prevents substantial movement of the carbon-centred radical species after hydrogen-atom transfer, precluding reorientation and rotation around the C_{phenyl}–$C_{tertiary}$ bond, thus avoiding an interconversion of the radical intermediates formed from (*R*)-**1a** and (*S*)-**1a** and ablation of enantioselectivity. In addition, for substrate (*R*)-**1a**, the ethyl substituent is placed in a sterically accessible area between residues P268 and V328, while the methyl group is oriented towards the outwards-facing side of the active site (see Supplementary Figs. 22–26 for details). By contrast, for the other enantiomer, (*S*)-**1a**, the ethyl substituent mostly rotates upwards to avoid an otherwise close contact of the CH_3 group of the ethyl substituent with the haem ring system. However, the rotation of the ethyl group causes a substantial movement of F437 and the respective open-loop protein backbone, which results in exclusion of (*S*)-**1a** from the enzyme pocket or a destabilization of the HAT transition state, thereby disfavouring reaction with (*S*)-**1a** (see Supplementary Figs. 22–26 for details). The computational results are consistent with the experimental findings based on the biotransformation of enantiomers (*R*)-**1f** (Fig. 4a) and (*S*)-**1f** (Fig. 4b).

Conclusions

We have developed an engineered enzyme, P411-TEA-5274, that can directly aminate tertiary C–H bonds, efficiently and selectively to produce high-value chiral α-tertiary primary amines. This biocatalyst provides an alternative to small-molecule catalysts, which struggle to functionalize tertiary C–H bonds, and demonstrates remarkable enantioselectivity and activity. The substrate scope study demonstrated the compatibility of this biotransformation towards various substrates, the exclusive regioselectivity to tertiary C–H bonds and the broad applicability against different tertiary C–H bonds. Experimental and computational investigations indicate that the enzyme's excellent enantioselectivity arises from its enantiomeric substrate specificity. Given the prevalence of α-tertiary amines in bioactive molecules, this work provides a straightforward disconnection strategy to construct these fragments. Leveraging this work in the future, we hope to expand the limited repertoire of catalysts for asymmetric intermolecular functionalization of tertiary C–H bonds.

Methods

Expression of P411-TEA variants

E. coli (*E. cloni* BL21(DE3)) cells carrying plasmid encoding the appropriate P411-TEA variant were grown overnight in 5 ml of Luria-Bertani

https://doi.org/10.1038/s41929-024-01149-w

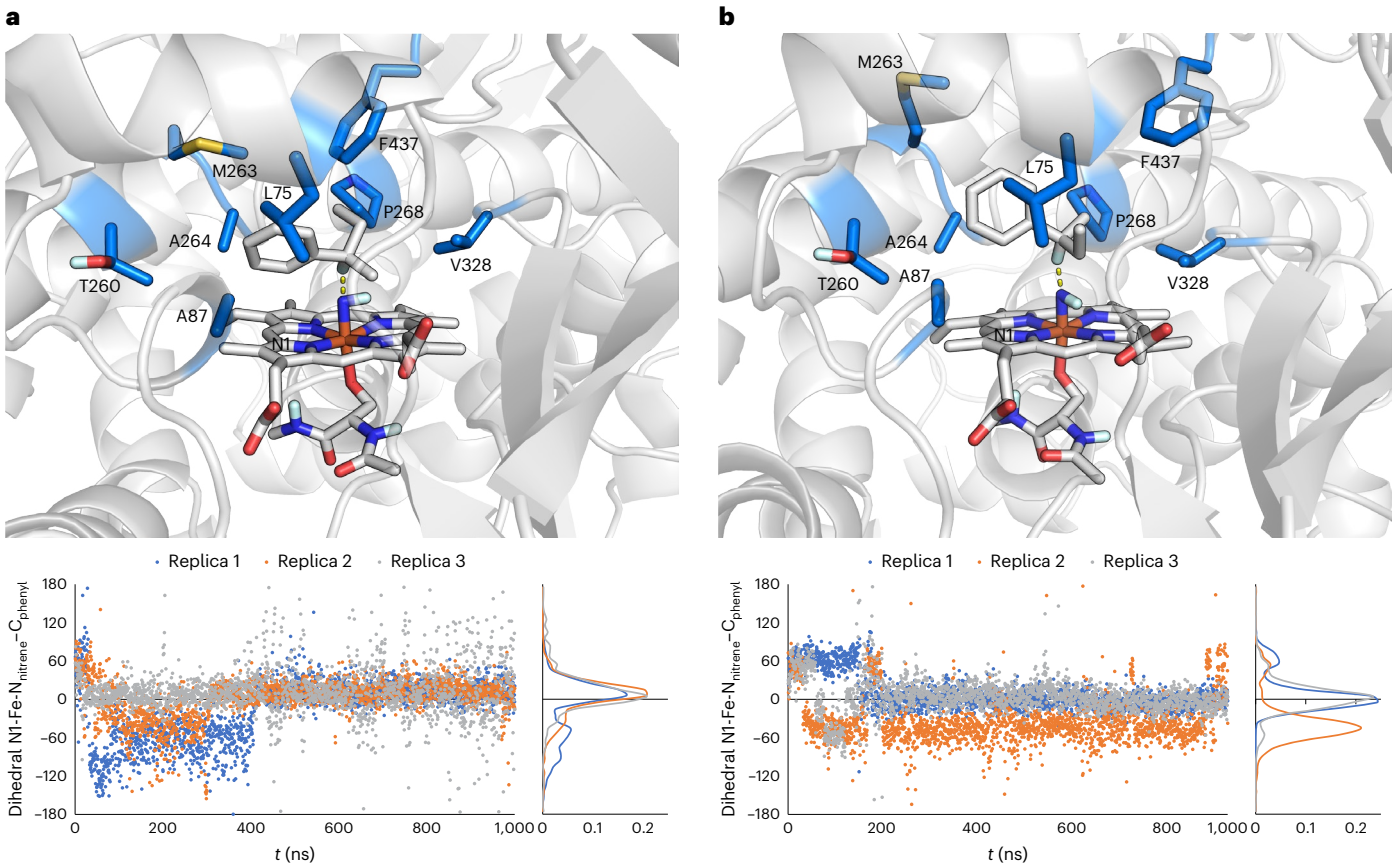

Fig. 5 | Molecular dynamics simulations of iron-haem-catalysed tertiary C–H amination. a,**b**, Molecular dynamics simulations of HAT transition state mimics with (*R*)-**1a** (**a**) and (*S*)-**1a** (**b**). Plot of the N1-Fe-$N_{nitrene}$–C_{phenyl} dihedral angle over time and respective probability density plot. During the simulations, the $N_{nitrene}$–H–$C_{tertiary}$ distance (dashed yellow line) was restrained. Structures correspond to representative structures of the most populated cluster. Non-relevant, non-polar hydrogens are omitted for clarity. The colour scheme for atoms of amino acid residues: carbon, blue; oxygen, red and sulfur, yellow; for the atoms of **1a** and the iron–nitrene intermediate: carbon, grey; iron, orange; nitrogen, blue and oxygen, red.

medium with 0.1 mg ml^{-1} ampicillin (LB_{amp}). Preculture (1 ml) was used to inoculate 50 ml of Hyper Broth medium with 0.1 mg ml^{-1} ampicillin (HB_{amp}) in an Erlenmeyer flask (125 ml). This culture was incubated at 37 °C and 220 rpm for 2.5 h, cooled on ice for 30 min, and induced with 0.5 mM isopropyl *β*-D-1-thiogalactopyranoside and 1.0 mM 5-aminolevulinic acid (final concentrations). Expression was conducted at 22 °C, 140 rpm for 20–22 h. *E. coli* cells were then transferred to a conical centrifuge tube (50 ml) and pelleted by centrifugation (4,000*g*, 3 min and 4 °C). Supernatant was removed and the resulting cell pellet was resuspended in M9-N (pH 8.0) buffer to an optical density at 600 nm (OD_{600}) of 38. An aliquot of this cell suspension (3 ml) was taken to determine protein concentration using the pyridine haemochromagen assay after lysis by sonication.

Primary amination of tertiary C–H bonds using whole *E. coli* cells harbouring P411-TEA

All the biocatalytic reactions were set up in an anaerobic chamber (oxygen level <40 ppm). M9-N medium (pH 8.0) and D-glucose solution (500 mM in M9-N, pH 8.0) were placed in the anaerobic chamber for at least 24 h. Collected cells were resuspended with M9-N buffer (pH 8.0) in to OD_{600} = 38 and 320 µl of resuspended cells were aliquoted to 2 ml screw-cap vials. The screw-cap vials with cells were precooled to 0 °C on an ice bath. Then, 30 µl of the precooled glucose solution, 10 µl of a stock solution containing glucose oxidase (from *Aspergillus niger*, 1,000 U ml^{-1}) and catalase (from bovine liver, 14,000 U ml^{-1}) in double-distilled water were added to make the total volume to 360 µl. The resulting mixtures stayed on the ice bath for another 2 min, and then the hydrocarbon substrate **1** (20 µl, 0.1 M stock in ethanol) and the nitrene precursor **2a** (20 µl, 0.2 M stock in water) were added in a sequential manner. The reactions were then shaken at 10 °C for 20 h at 250 rpm.

Reporting summary

Further information on research design is available in the Nature Portfolio Reporting Summary linked to this article.

Data availability

Crystallographic data are available free of charge from the Cambridge Crystallographic Data Centre under no. CCDC 2287786 (**3f** derivative (*S*)-*N*-(2-(4-methoxyphenyl)butan-2-yl)benzamide). The original materials and data that support the findings of this study are available within the paper and its Supplementary Information or can be obtained from the corresponding author upon reasonable request.

References

1. Chu, J. C. K. & Rovis, T. Complementary strategies for directed C(sp^3)–H functionalization: a comparison of transition-metal-catalyzed activation, hydrogen atom transfer, and carbene/nitrene transfer. *Angew. Chem. Int. Ed.* **57**, 62–101 (2018).
2. Dalton, T., Faber, T. & Glorius, F. C–H activation: toward sustainability and applications. *ACS Cent. Sci.* **7**, 245–261 (2021).
3. Newton, C. G., Wang, S. G., Oliveira, C. C. & Cramer, N. Catalytic enantioselective transformations involving C–H bond cleavage by transition-metal complexes. *Chem. Rev.* **117**, 8908–8976 (2017).

4. Saint-Denis, T. G., Zhu, R. Y., Chen, G., Wu, Q. F. & Yu, J. Q. Enantioselective C(sp^3)–H bond activation by chiral transition metal catalysts. *Science* **359**, eaao4798 (2018).
5. Rogge, T. et al. C–H activation. *Nat. Rev. Methods Primers* **1**, 43 (2021).
6. Davies, H. M. L. & Beckwith, R. E. J. Catalytic enantioselective C–H activation by means of metal-carbenoid-induced C–H insertion. *Chem. Rev.* **103**, 2861–2904 (2003).
7. Zhang, C., Li, Z. L., Gu, Q. S. & Liu, X. Y. Catalytic enantioselective C(sp^3)–H functionalization involving radical intermediates. *Nat. Commun.* **12**, 475 (2021).
8. Yang, Y. & Arnold, F. H. Navigating the unnatural reaction space: directed evolution of heme proteins for selective carbene and nitrene transfer. *Acc. Chem. Res.* **54**, 1209–1225 (2021).
9. Zhang, R. K., Huang, X. & Arnold, F. H. Selective C–H bond functionalization with engineered heme proteins: new tools to generate complexity. *Curr. Opin. Chem. Biol.* **49**, 67–75 (2019).
10. Lewis, J. C., Coelho, P. S. & Arnold, F. H. Enzymatic functionalization of carbon–hydrogen bonds. *Chem. Soc. Rev.* **40**, 2003–2021 (2011).
11. Yang, Y., Cho, I., Qi, X., Liu, P. & Arnold, F. H. An enzymatic platform for the asymmetric amination of primary, secondary and tertiary C(sp^3)–H bonds. *Nat. Chem.* **11**, 987–993 (2019).
12. Yang, C.-J. et al. Cu-catalysed intramolecular radical enantioconvergent tertiary β-C(sp^3)–H amination of racemic ketones. *Nat. Catal.* **3**, 539–546 (2020).
13. Lang, K., Li, C., Kim, I. & Zhang, X. P. Enantioconvergent amination of racemic tertiary C–H bonds. *J. Am. Chem. Soc.* **142**, 20902–20911 (2020).
14. Ye, C. X., Shen, X., Chen, S. & Meggers, E. Stereocontrolled 1,3-nitrogen migration to access chiral α-amino acids. *Nat. Chem.* **14**, 566–573 (2022).
15. Ye, C.-X., Dansby, D. R., Chen, S. & Meggers, E. Expedited synthesis of α-amino acids by single-step enantioselective α-amination of carboxylic acids. *Nat. Synth.* **2**, 645–652 (2023).
16. Hahn, C. J. et al. Crystal structure of a key enzyme for anaerobic ethane activation. *Science* **373**, 118–121 (2021).
17. Zanger, U. M. & Schwab, M. Cytochrome P450 enzymes in drug metabolism: regulation of gene expression, enzyme activities, and impact of genetic variation. *Pharmacol. Ther.* **138**, 103–141 (2013).
18. Huang, X. & Groves, J. T. Oxygen activation and radical transformations in heme proteins and metalloporphyrins. *Chem. Rev.* **118**, 2491–2553 (2018).
19. Poulos, T. L. Cytochrome P450 flexibility. *Proc. Natl Acad. Sci. USA* **100**, 13121–13122 (2003).
20. Brandenberg, O. F., Fasan, R. & Arnold, F. H. Exploiting and engineering hemoproteins for abiological carbene and nitrene transfer reactions. *Curr. Opin. Biotechnol.* **47**, 102–111 (2017).
21. Chen, K. & Arnold, F. H. Engineering new catalytic activities in enzymes. *Nat. Catal.* **3**, 203–213 (2020).
22. Hager, A., Vrielink, N., Hager, D., Lefranc, J. & Trauner, D. Synthetic approaches towards alkaloids bearing α-tertiary amines. *Nat. Prod. Rep.* **33**, 491–522 (2016).
23. Liu, G., Cogan, D. A. & Ellman, J. A. Catalytic asymmetric synthesis oftert-butanesulfinamide. Application to the asymmetric synthesis of amines. *J. Am. Chem. Soc.* **119**, 9913–9914 (1997).
24. Ellman, J. A., Owens, T. D. & Tang, T. P. *N-tert*-butanesulfinyl imines: versatile intermediates for the asymmetric synthesis of amines. *Acc. Chem. Res.* **35**, 984–995 (2002).
25. Gao, X., Turek-Herman, J. R., Choi, Y. J., Cohen, R. D. & Hyster, T. K. Photoenzymatic synthesis of α-tertiary amines by engineered flavin-dependent 'ene'-reductases. *J. Am. Chem. Soc.* **143**, 19643–19647 (2021).
26. Barrios-Rivera, J., Xu, Y., Wills, M. & Vyas, V. K. A diversity of recently reported methodology for asymmetric imine reduction. *Org. Chem. Front.* **7**, 3312–3342 (2020).
27. Slabu, I., Galman, J. L., Lloyd, R. C. & Turner, N. J. Discovery, engineering, and synthetic application of transaminase biocatalysts. *ACS Catal.* **7**, 8263–8284 (2017).
28. Afanasyev, O. I., Kuchuk, E., Usanov, D. L. & Chusov, D. Reductive amination in the synthesis of pharmaceuticals. *Chem. Rev.* **119**, 11857–11911 (2019).
29. Jia, Z. J., Gao, S. & Arnold, F. H. Enzymatic primary amination of benzylic and allylic C(sp^3)–H bonds. *J. Am. Chem. Soc.* **142**, 10279–10283 (2020).
30. Liu, Z. et al. An enzymatic platform for primary amination of 1-aryl-2-alkyl alkynes. *J. Am. Chem. Soc.* **144**, 80–85 (2022).
31. Yang, Y., Shi, S.-L., Niu, D., Liu, P. & Buchwald, S. L. Catalytic asymmetric hydroamination of unactivated internal olefins to aliphatic amines. *Science* **349**, 62–66 (2015).
32. Fandrick, K. R. et al. A general copper-BINAP-catalyzed asymmetric propargylation of ketones with propargyl boronates. *J. Am. Chem. Soc.* **133**, 10332–10335 (2011).
33. Kille, S. et al. Reducing codon redundancy and screening effort of combinatorial protein libraries created by saturation mutagenesis. *ACS Synth. Biol.* **2**, 83–92 (2013).
34. Reetz, M. T. & Carballeira, J. D. Iterative saturation mutagenesis (ISM) for rapid directed evolution of functional enzymes. *Nat. Protoc.* **2**, 891–903 (2007).
35. Prier, C. K., Zhang, R. K., Buller, A. R., Brinkmann-Chen, S. & Arnold, F. H. Enantioselective, intermolecular benzylic C–H amination catalysed by an engineered iron-haem enzyme. *Nat. Chem.* **9**, 629–634 (2017).
36. D'Amato, E. M., Borgel, J. & Ritter, T. Aromatic C–H amination in hexafluoroisopropanol. *Chem. Sci.* **10**, 2424–2428 (2019).
37. Legnani, L., Prina Cerai, G. & Morandi, B. Direct and practical synthesis of primary anilines through iron-catalyzed C–H bond amination. *ACS Catal.* **6**, 8162–8165 (2016).
38. Liu, J. et al. Fe-catalyzed amination of (hetero)arenes with a redox-active aminating reagent under mild conditions. *Eur. J. Chem.* **23**, 563–567 (2017).
39. Luo, Y.-R. *Comprehensive Handbook of Chemical Bond Energies* (Taylor & Francis, 2007).
40. Pan, Y. et al. Kinetic resolution of α-tertiary propargylic amines through asymmetric remote aminations of anilines. *ACS Catal.* **11**, 8443–8448 (2021).
41. Hennessy, E. T., Liu, R. Y., Iovan, D. A., Duncan, R. A. & Betley, T. A. Iron-mediated intermolecular *N*-group transfer chemistry with olefinic substrates. *Chem. Sci.* **5**, 1526–1532 (2014).
42. Jacobs, B. P., Wolczanski, P. T., Jiang, Q., Cundari, T. R. & MacMillan, S. N. Rare examples of Fe(IV) alkyl-imide migratory insertions: impact of Fe–C covalency in (Me_2IPr)Fe(=NAd)R_2 (R=^{neo}Pe, 1-nor). *J. Am. Chem. Soc.* **139**, 12145–12148 (2017).
43. Singh, R., Kolev, J. N., Sutera, P. A. & Fasan, R. Enzymatic C(sp^3)–H amination: P450-catalyzed conversion of carbonazidates into oxazolidinones. *ACS Catal.* **5**, 1685–1691 (2015).
44. Athavale, S. V. et al. Enzymatic nitrogen insertion into unactivated C–H bonds. *J. Am. Chem. Soc.* **144**, 19097–19105 (2022).

Acknowledgements

This work is supported by the National Institute of General Medical Science of the National Institutes of Health (grant no. R01GM138740). Support by National Science Foundation Division of Chemistry (grant no. CHE-2153972 to K.N.H.) and the Alexander von Humboldt-Foundation (Feodor Lynen Fellowship, T.R.) is gratefully acknowledged. We thank S. C. Virgil for the maintenance of the Caltech Center for Catalysis and Chemical Synthesis (3CS). We thank M. Shahgoli for mass spectrometry assistance. We thank D. Vander Velde for the maintenance of the Caltech nuclear magnetic resonance

facility. We thank M. K. Takase and L. M. Henling for assistance with X-ray crystallographic data collection. We also thank S. Brinkmann-Chen for the helpful discussions and comments on the manuscript.

Author contributions

R.M. conceptualized and designed the project under the guidance of F.H.A. R.M. and S.G. carried out the initial screening of haem proteins. R.M., S.G. and S.J.W. performed the directed evolution experiments, with support from Z.-Y.Q. for the validation. R.M., S.G. and Z.-Y.Q. investigated the substrate scope and reaction mechanism, with support from Z.-Q.L. T.R. carried out the computational studies with K.N.H. providing guidance. A.D. conducted crystallization of a **3f** derivative. R.M. and F.H.A. wrote the manuscript with input from all authors.

Competing interests

The authors declare no competing interests.

Additional information

Supplementary information The online version contains supplementary material available at https://doi.org/10.1038/s41929-024-01149-w.

Correspondence and requests for materials should be addressed to Frances H. Arnold.

Peer review information *Nature Catalysis* thanks Bernhard Hauer, Nicholas Turner and the other, anonymous, reviewer(s) for their contribution to the peer review of this work.

nature portfolio

Corresponding author(s): Frances H. Arnold

Last updated by author(s): Feb 7, 2024

Reporting Summary

Nature Portfolio wishes to improve the reproducibility of the work that we publish. This form provides structure for consistency and transparency in reporting. For further information on Nature Portfolio policies, see our Editorial Policies and the Editorial Policy Checklist.

Statistics

For all statistical analyses, confirm that the following items are present in the figure legend, table legend, main text, or Methods section.

n/a	Confirmed	
☒	☐	The exact sample size (*n*) for each experimental group/condition, given as a discrete number and unit of measurement
☒	☐	A statement on whether measurements were taken from distinct samples or whether the same sample was measured repeatedly
☒	☐	The statistical test(s) used AND whether they are one- or two-sided *Only common tests should be described solely by name; describe more complex techniques in the Methods section.*
☒	☐	A description of all covariates tested
☒	☐	A description of any assumptions or corrections, such as tests of normality and adjustment for multiple comparisons
☒	☐	A full description of the statistical parameters including central tendency (e.g. means) or other basic estimates (e.g. regression coefficient) AND variation (e.g. standard deviation) or associated estimates of uncertainty (e.g. confidence intervals)
☒	☐	For null hypothesis testing, the test statistic (e.g. *F*, *t*, *r*) with confidence intervals, effect sizes, degrees of freedom and *P* value noted *Give P values as exact values whenever suitable.*
☒	☐	For Bayesian analysis, information on the choice of priors and Markov chain Monte Carlo settings
☒	☐	For hierarchical and complex designs, identification of the appropriate level for tests and full reporting of outcomes
☒	☐	Estimates of effect sizes (e.g. Cohen's *d*, Pearson's *r*), indicating how they were calculated

Our web collection on statistics for biologists contains articles on many of the points above.

Software and code

Policy information about availability of computer code

Data collection	Amber 16; AmberTools 21; AmberTools 16; Gaussian 09, Rev D.01
Data analysis	AmberTools 21; AmberTools 16; PyMOL v. 1.8.2.; Microsoft Excel 2016; GaussView 6

For manuscripts utilizing custom algorithms or software that are central to the research but not yet described in published literature, software must be made available to editors and reviewers. We strongly encourage code deposition in a community repository (e.g. GitHub). See the Nature Portfolio guidelines for submitting code & software for further information.

Data

Policy information about availability of data

All manuscripts must include a data availability statement. This statement should provide the following information, where applicable:

- Accession codes, unique identifiers, or web links for publicly available datasets
- A description of any restrictions on data availability
- For clinical datasets or third party data, please ensure that the statement adheres to our policy

A data availability statement has been provided in the manuscript.

Human research participants

Policy information about studies involving human research participants and Sex and Gender in Research.

Reporting on sex and gender	N/A
Population characteristics	N/A
Recruitment	N/A
Ethics oversight	N/A

Note that full information on the approval of the study protocol must also be provided in the manuscript.

Field-specific reporting

Please select the one below that is the best fit for your research. If you are not sure, read the appropriate sections before making your selection.

☐ Life sciences ☐ Behavioural & social sciences ☐ Ecological, evolutionary & environmental sciences

For a reference copy of the document with all sections, see nature.com/documents/nr-reporting-summary-flat.pdf

Life sciences study design

All studies must disclose on these points even when the disclosure is negative.

Sample size	N/A
Data exclusions	N/A
Replication	N/A
Randomization	N/A
Blinding	N/A

Behavioural & social sciences study design

All studies must disclose on these points even when the disclosure is negative.

Study description	N/A
Research sample	N/A
Sampling strategy	N/A
Data collection	N/A
Timing	N/A
Data exclusions	N/A
Non-participation	N/A
Randomization	N/A

Ecological, evolutionary & environmental sciences study design

All studies must disclose on these points even when the disclosure is negative.

Study description	N/A
Research sample	N/A
Sampling strategy	N/A
Data collection	N/A
Timing and spatial scale	N/A
Data exclusions	N/A
Reproducibility	N/A
Randomization	N/A
Blinding	N/A

Did the study involve field work? ☐ Yes ☒ No

Reporting for specific materials, systems and methods

We require information from authors about some types of materials, experimental systems and methods used in many studies. Here, indicate whether each material, system or method listed is relevant to your study. If you are not sure if a list item applies to your research, read the appropriate section before selecting a response.

Materials & experimental systems

n/a	Involved in the study
☒	☐ Antibodies
☒	☐ Eukaryotic cell lines
☒	☐ Palaeontology and archaeology
☒	☐ Animals and other organisms
☒	☐ Clinical data
☒	☐ Dual use research of concern

Methods

n/a	Involved in the study
☒	☐ ChIP-seq
☒	☐ Flow cytometry
☒	☐ MRI-based neuroimaging